# Cytokine Induction during T-Cell-Mediated Clearance of Mouse Hepatitis Virus from Neurons In Vivo†

B. D. PEARCE, M. V. HOBBS, T. S. McGRAW, AND M. J. BUCHMEIER*

*The Scripps Research Institute, La Jolla, California 92037*

To investigate the mechanism by which viruses are cleared from neurons in the central nervous system, we have utilized a mouse model involving infection with a neurotropic variant of mouse hepatitis virus (OBLV60). After intranasal inoculation, OBLV60 grew preferentially in the olfactory bulbs of BALB/c mice. Using in situ hybridization, we found that viral RNA localized primarily in the outer layers of the olfactory bulb, including neurons of the mitral cell layer. Virus was cleared rapidly from the olfactory bulb between 5 and 11 days. Athymic nude mice failed to eliminate the virus, demonstrating a requirement for T lymphocytes. Immunosuppression of normal mice with cyclophosphamide also prevented clearance. Both CD4$^+$ and CD8$^+$ T-cell subsets were important, as depletion of either of these subsets delayed viral clearance. Gliosis and infiltrates of CD4$^+$ and CD8$^+$ cells were detected by immunohistochemical analysis at 6 days. The role of cytokines in clearance was investigated by using an RNase protection assay for interleukin-1α (IL-1α), IL-1β, IL-2, IL-3, IL-4, IL-5, IL-6, tumor necrosis factor alpha (TNF-α), TNF-β, and gamma interferon (IFN-γ). In immunocompetent mice there was upregulation of RNA for IL-1α, IL-1β, IL-6, TNF-α, and IFN-γ at the time of clearance. Nude mice had comparable increases in these cytokine messages, with the exception of IFN-γ. Induction of major histocompatibility complex class I (MHC-I) molecules on cells in infected brains was demonstrated by immunohistochemical analyses in normal and nude mice, suggesting that IFN-γ may not be necessary for induction of MHC-I on neural cells in vivo.

After a virus has entered the central nervous system (CNS) there are several possible outcomes, depending on the interaction between the virus and the host immune system (59). Fulminate encephalitis results when virus spreads too rapidly to be contained by an unprimed or ineffectual immune system. At the opposite extreme, a virus may cause minimal cytopathologic change and establish a persistent infection (49). Although the CNS has historically been considered an immunologically privileged site, viral infections can nevertheless be controlled through antibody- or cell-mediated mechanisms (41, 50, 52). The mechanisms of T-cell-mediated clearance are poorly understood but are likely to differ from those employed in the periphery, because the CNS lacks lymphatic ducts and constitutive major histocompatibility complex class I (MHC-I) expression and its vascular architecture imposes constraints on access by leukocytes and soluble immune mediators (10). Furthermore, as most CNS neurons are terminally differentiated, nondividing cells, clearance of virus by a noncytopathic mechanism is advantageous. Clearly, a detailed understanding of the immune mechanisms responsible for viral clearance in the CNS is needed in order to develop therapeutic strategies to limit or prevent neuronal damage as a result of acute and chronic viral encephalitides.

Mouse hepatitis virus (MHV), a member of the coronavirus family, has been used to study virus-induced neurological diseases. In the murine model, the outcome of infection depends on the virus strain and route of inoculation as well as on host responses and genetic susceptibility (9). While several important studies have examined the clearance of MHV from the murine CNS, there are drawbacks to each of the models

employed. For example, studies using intracranial inoculations (51, 62, 63, 68, 71) compromise the blood-brain barrier, confound studies of viral spread, and influence the entry of immune cells or soluble mediators into the CNS. Conversely, intranasal inoculation with hepatotropic strains of MHV, which are normally spread by a fecal-oral route, cause hepatitis which can be fatal and might complicate studies of the immune response to the CNS infection (3, 9). Neurovirulent strains produce an acute and often fatal encephalitis with extensive neuronal involvement, whereas neuroattenuated strains spread only slowly in neurons and generally infect glia, with attendant chronic white matter disease (7, 15, 17, 33). In the study of viral clearance from neurons, it is advantageous to have a model in which neurons are infected preferentially but in which fatal encephalitis does not ensue. The recently isolated JHM-CC small-plaque mutant (27) and the V5A13.1 deletion mutant (13) partially fulfill these requirements, but these MHV variants appear to persist in white matter (12a, 27). These studies underscore the need for a model of MHV clearance from the CNS in which the variables responsible for clearance can be more easily isolated and identified. In such a model, clearance would ideally be rapid and complete, with minimal white matter degeneration.

Although data derived from available models has implicated both CD4$^+$ and CD8$^+$ cells in clearing MHV from the CNS (48, 63, 68, 71), the mechanisms underlying this process are enigmatic. Fatal MHV encephalitis can be prevented by adoptive transfer of CD4$^+$ cells, without significantly decreasing viral load (62). Conversely, immune-competent mice inoculated with MHV (JMHV-DS) intracerebrally succumb to the infection even though viral titers in the brain have declined to undetectable levels (67). Several reports have focused attention on cytokines as possible mediators of MHV clearance (48, 63, 66, 71), yet in part because of technical limitations, there is a lack of studies involving direct measurements of cytokines induced in the CNS during clearance of MHV.

* Corresponding author. Mailing address: Department of Neuropharmacology, The Scripps Research Institute CVN 8, 10666 N. Torrey Pines Rd., La Jolla, CA 92037. Phone: (619) 554-7056. Fax: (619) 554-6470.
† Scripps Research Institute manuscript no. 8455-NP.

One impediment to direct measurements of cytokines in serum or tissue is that the assays employed may be too insensitive to detect small changes in cytokine levels (61). Nevertheless, gamma interferon (IFN-γ) has been strongly implicated in viral clearance on the basis of indirect indices of cytokine induction (43, 54, 61, 66). Moreover, MHV infection differentially regulates spleen cell production of IFN-γ and that of interleukin-2 (IL-2), IL-3, and IL-4 (10a, 37). It is not known if there is a similar modulation of the immune cells infiltrating MHV-infected brain tissue in vivo, but T cells derived from the brains of infected mice produce IFN-γ and IL-2 after stimulation in vitro (66). There is a complex interregulation of these and other cytokines which are probably operating together as a network during viral clearance (5, 54). A thorough appreciation of the operation of this network during clearance of viruses from the CNS will likely require analysis of the temporal sequence of induction for each of the cytokines involved in the clearance process.

In this report, we describe a mouse model developed to overcome some of the limitations to studying MHV clearance from the CNS. This model utilizes intranasal infection with an MHV variant (OBLV60) which is highly neurotropic yet manifests distinct and limited regional localization within the brain, low mortality, and no paralytic sequela. We have used this model to assess the temporal pattern of induction of 10 different cytokine genes during viral clearance. We further correlate the pattern of cytokine gene induction with macrophage and T-cell infiltration, gliosis, and the expression of immune accessory molecules of MHC-I and MHC-II.

## MATERIALS AND METHODS

**Virus and infection protocol.** Virus stocks were grown in OBL-21a cells (55) from a 60-day isolate designated OBLV60, as described previously (19). MHV4 was propagated in Sac⁻ cells (19). Mice (7 to 13 weeks old) were inoculated with 1,000 PFU of OBLV60 intranasally and then killed by exsanguination under methoxyflurane or ketamine anesthesia. Sham-inoculated mice served as controls. Virus titers in tissue homogenates or cell supernatants were determined by plaque assay on DBT cells, as described previously (13). For studies of virus-induced syncytia, the hypothalamic neuron cell line, GT1-7 (gift of P. J. Mellon) (47), was grown in six-well culture plates and infected with approximately 0.5 PFU per cell of either OBLV60 or MHV4 diluted in Dulbecco modified Eagle medium containing 10% fetal calf serum. Control cultures received medium only. Cultures were observed and photographed under phase-contrast microscopy.

**Depletion of T-cell subsets.** Clarified ascites containing anti-L3T4 (GK 1.5) (gift of Rolf Kiessling) or anti-Lyt 2.2 (19-1.78) (gift of Gunther Hammerling) monoclonal antibodies (MAb) were used, respectively, to deplete CD4⁺ or CD8⁺ T cells. Mice used for in situ hybridization studies were given 0.2 ml of MAb intraperitoneally 1 day prior to infection and were given a booster injection with 0.2 ml of MAb on the day of infection and 4 days after infection. Mice used in plaquing studies were given 0.2 ml of MAb 1 day prior to infection and were then given booster injections with 0.2 ml of MAb on days 2, 10, 16, and 25 postinfection. When mice were doubly depleted of both subsets, 0.2 ml of each MAb was used at the times indicated above. Depletion of T-cell subsets was confirmed by fluorescence-activated cell sorter analysis of splenocytes from mice at 16 days postinfection. In CD8⁺ cell-depleted mice, only 0.3% of cells were CD8⁺; in CD4⁺-depleted mice, 1.3% of cells were CD4⁺.

**In situ hybridization.** In situ hybridization to detect viral RNA was performed as described previously (13). Briefly, the hybridization procedure was performed on zinc formalin-fixed, paraffin-embedded sections. The radiolabeled ([³⁵S]ATP and [³⁵S]CTP) RNA probe which was used in this procedure was derived by in vitro transcription (Gemini II kit; Promega) and is antisense to a 1.8-kb 3' fragment of the MHV-A59 genome. This probe has been used successfully to localize RNA for several stains of MHV (13). The tissue was treated with 10 μg of proteinase K per ml to improve probe accessibility and removal. When immunohistochemistry preceded the in situ procedure, 100 μg of proteinase K per ml was used. The probe was hybridized overnight at 55°C, and unhybridized probe was then digested with RNase A. Sections were rinsed several times in SSC (1× SSC is 0.15 M NaCl plus 0.015 M sodium citrate) before being dehydrated through graded alcohols and placed on Cronex film (Dupont). Cellular localization of signal was performed on slides coated with NTB2 radiosensitive emulsion (Kodak).

**Immunohistochemistry.** The following antibodies were used for immunohistochemical analyses (diluted in phosphate-buffered saline): anti-bovine glial fibrillary acidic protein (rabbit polyclonal anti-GFAP; Dakopatts), 1:200; anti-nonphospho-neurofilament protein (mouse MAb SMI 311; Sternberger Monoclonals), 1:1000; anti-CD4 (rat MAb L3T4; Pharmingen), 1:50; anti-CD8 (rat MAb Ly-2 and Ly-3; Pharmingen), 1:50; anti-H-2 mouse monotypic antigen (rat MAb M1/42; Boehringer Mannheim), 1:20; anti-IA$^d$ (biotin-conjugated mouse MAb AMS32.1; Pharminigen), 1:50; anti-F4/80 (C1: A3-1; Serotec), 1:10; anti-H-2K$^d$ (biotin-conjugated mouse MAb SF-1.1; Pharmingen), 1:200; anti-H-2K$^b$ (biotin-conjugated mouse MAb AF6-88.5; Pharmingen), 1:200. When the primary antibody was not biotinylated, a biotinylated secondary antibody was used (Vector Laboratories).

Immunohistochemical analyses for GFAP, F4/80, and non-phosoneurofilament protein were performed on tissues fixed in zinc formalin (Anatech) which were then embedded in paraffin. Staining for CD4, CD8, H-2 monotyptic, or IA$^d$ cells was performed on frozen sections fixed in acetone or ethanol at −20°C. Ethanol gave superior fixation but increased background staining compared with acetone fixation. Acetone-fixed frozen sections were used for F4/80 and H-2K$^d$ staining. When using these two antibodies, fixation in 2% paraformaldehyde improved morphology without diminishing staining intensity. Aldehyde fixation of tissue prior to immunostaining with F4/80 necessitated treatment with trypsin to reveal epitopes. Normal goat serum, avidin/biotin (Vector Laboratories), and 1% hydrogen peroxide in methanol were used as needed to block nonspecific staining. The ABC elite staining system was used according to the manufacturer's instructions (Vector Laboratories). Diaminobenzidine was used as a chromogen, and all slides were counterstained with hematoxylin.

When combining immunohistochemical analysis to identify neurons with in situ hybridization for viral RNA, the above procedure was modified. Immunohistochemical analysis for nonphosoneurofilament proteins preceded in situ hybridization and utilized a buffer intended to reduce RNase activity and loss of in situ signal (26). The immunohistochemical analysis was performed in 0.05 M Tris (pH 7.6) containing 1.5% (wt/vol) NaCl. During incubations with antibodies, 0.2 mg of tRNA per ml–5,000 U of sodium heparin per ml was included in the buffer. After applying diaminobenzidine, slides were dehydrated by passage through alcohol and stored for up to 48 h prior to undergoing the in situ procedure.

**RNase protection assay.** Total RNA was isolated from mouse brain tissues by extraction in guanidinium thiocyanate followed by centrifugation through 5.7 M CsCl (56). The
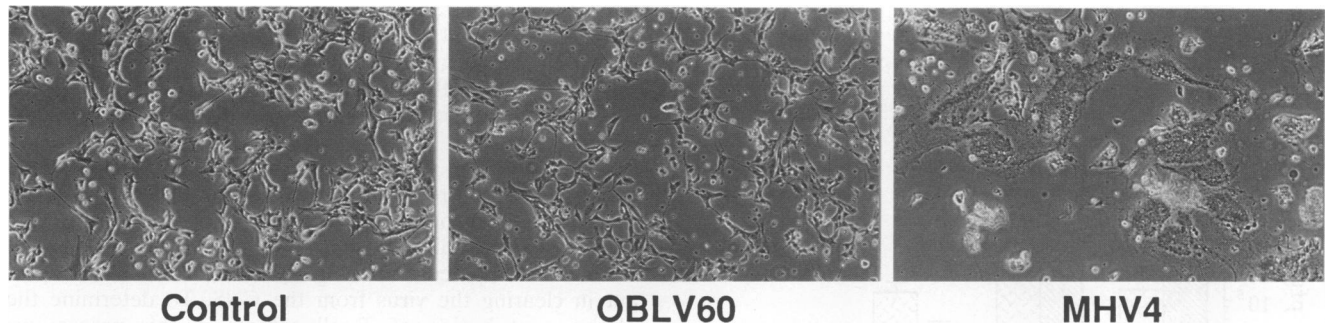
FIG. 1. OBLV60 does not induce syncytia in the neuron cell line, GT1-7. The parental virus, MHV4, readily causes syncytia in these cells. Representative cultures are shown at 24 h after inoculation. The titer of OBLV60 in supernatant was $2.0 \times 10^7$ PFU per ml versus $4.4 \times 10^5$ PFU per ml for MHV4. Original magnification, $\times 100$.

RNase protection assay for quantitation of cytokine mRNA was performed exactly as described previously (25). The mIL-1$\alpha$(B), mIL-1$\beta$(A), mIL-2(A), mIL-3(B), mIL-4(B), mIL-5(C), mIL-6(B), mIFN$\gamma$(B), mTNF$\alpha$(A), mTNF$\beta$(A), and mL32(A) subclones in pGEM-4 (described in a previous report [25]) were linearized with EcoRI and were used as a set for T7-directed synthesis of $^{32}$P-labeled antisense RNA probes. The hybridization reactions (5 µg of target RNA), RNase treatments, isolation of protected RNA duplexes, and resolution of protected probes by denaturing polyacrylamide gels were as described previously (25). Within each assay, control groups included the probe set hybridized to tRNA only and to tRNA plus an equimolar pool of synthetic-sense RNAs complementary to the probe set. Dried gels were placed on film (XAR; Kodak) with intensifying screens and were developed for various periods of time at $-70°$C.

## RESULTS

OBLV60 is a variant of MHV4 which was isolated for its ability to grow in a transformed neuron-like cell line (OBL-21a) derived from the mouse olfactory bulb (19). This virus grows to high titer in OBL-21a cells and can persistently infect these cells without causing cytopathic effects (19). We investigated the ability of this virus to grow in a transformed neuron cell line (GT1-7) derived from the mouse hypothalamus (47). Although OBLV60 grew to higher titers in these cells than did MHV4, syncytia were evident in MHV4-infected cultures, whereas no syncytia were observed in OBLV60-infected cultures (Fig. 1). By 48 h after infection, few intact cells remained in the MHV4-infected cultures. In OBLV60-infected cultures, cells were reduced by 50 to 60% at this time, but no syncytia were observed. These data indicate that OBLV60 can infect neurons in vitro yet has reduced cytopathicity relative to the parental wild-type virus.

We therefore assessed the ability of OBLV60 to infect neurons in vivo by inoculating BALB/c mice with the virus intranasally and using in situ hybridization to determine the cellular localization of viral RNA. Most of the infected cells at 5 and 7 days postinoculation were found in the olfactory bulb and adjacent regions (Fig. 2). The glomerular and mitral layers were prominently involved, but infected cells were only occasionally seen in the internal granular layer. There was also frequent infection in the region of the ventral tegmentum. Infection of neurons in the olfactory bulb and ventral tegmentum was confirmed with in situ hybridization for viral RNA performed in conjunction with immunohistochemical analysis for neurofilament protein (data not shown). Infected cells were

occasionally seen elsewhere in the brain, including the habenula, septum, and brain stem; the hippocampus and cerebellum were consistently spared. Although the pattern of infection indicated predominant involvement of neurons, some glia may have also been infected.

Whereas intranasal inoculation with MHV4 usually resulted in fatal encephalitis as a result of widespread dissemination of infection in the brain (13), mice consistently recovered from infection with OBLV60. We therefore examined whether the virus was being cleared from the brains of OBLV60-infected mice during clinical recovery. Because in situ hybridization had revealed a predilection for the olfactory bulb, we compared viral titers in the olfactory bulb with titers in the remainder of the brain (Fig. 3A). Virus grew preferentially in the olfactory bulb, with peak titers in the olfactory bulb and the remainder of the brain occurring at 5 days postinfection. Titers declined rapidly to below detectable limits by 11 days. In situ hybridization, which detects viral RNA, was used to confirm that clearance was complete by 11 days postinfection (Fig. 4A). We detected no infected cells by microscopic examination of brain sections from these immunocompetent mice. In contrast, there was disseminated infection in the brains of mice which had
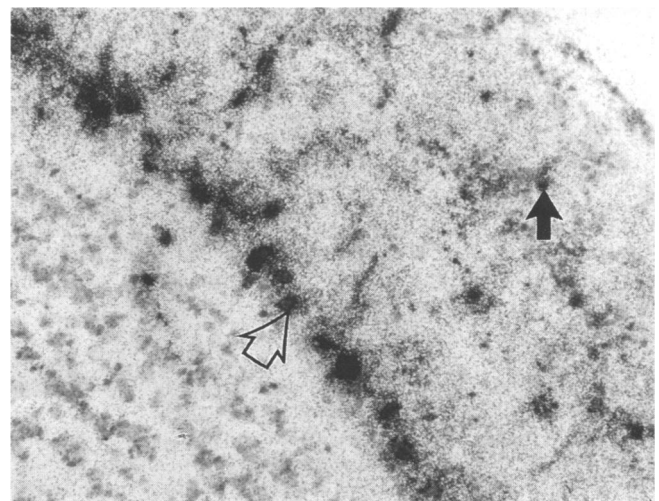


FIG. 2. In situ hybridization showing the distribution of viral RNA in the olfactory bulb 5 days after intranasal inoculation with OBLV60. Most infected cells are in the mitral (open arrow) and glomerular (solid arrow) cell layers, with relatively few infected cells in the internal granular cell layer. Original magnification, $\times 200$.
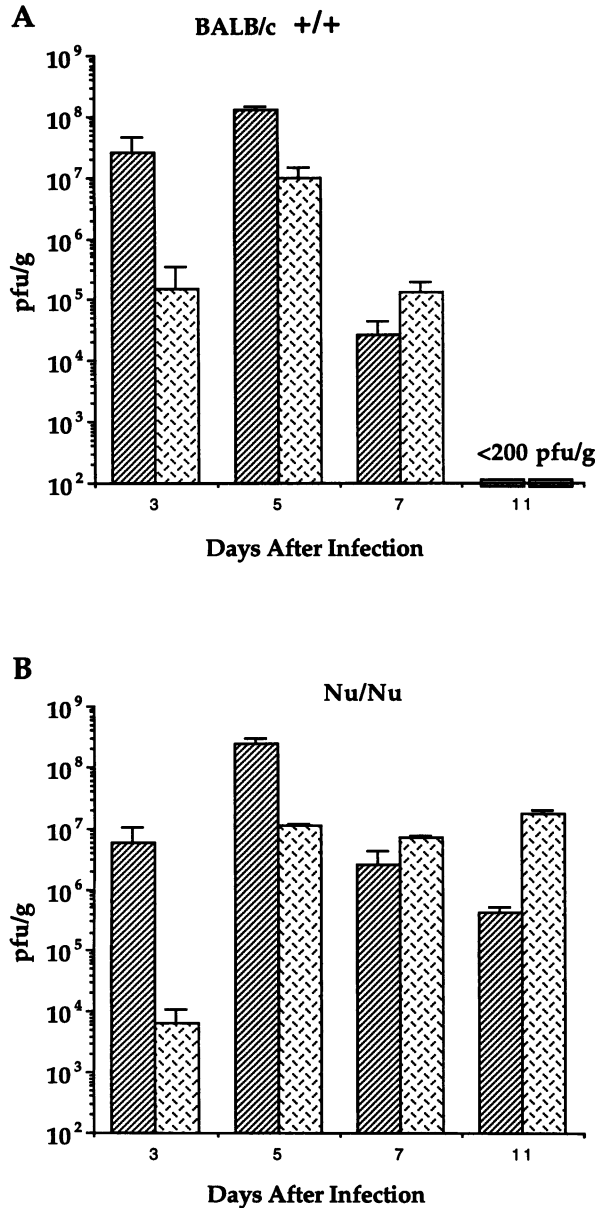
A



B



FIG. 3. Clearance of OBLV60 in normal and athymic nude mice. (A) Virus was cleared to below the limit of detection (200 PFU per g) in the olfactory bulb (hatched bars) and the remainder of the brain (stippled bars) by 11 days after infection in normal BALB/c mice. (B) Virus remained in the olfactory bulb (hatched bars) and the remainder of the brain (stippled bars) in immune-compromised mice. Mean virus titers are shown from groups of three mice; error bars are standard deviations.

been immune suppressed by the administration of cyclophosphamide at the time of inoculation (Fig. 4B). These immunosuppressed mice manifested signs of encephalitis and were moribund by 15 days postinfection, whereas infected immunocompetent controls were clinically normal at this time. Infected cells could not be found in the brains of initially immunocompetent mice which were then immunosuppressed with a single dose of cyclophosphamide at 24 days postinfection and evaluated at 31 days postinfection (Fig. 4C). These data further confirm that clearance was complete. Furthermore, we have

observed no symptoms of paralysis in any of the immune-competent infected mice, including a group of seven mice observed for a period of more than 1 year.

The role of T cells in mediating clearance was investigated by infecting BALB/c nu/nu (athymic nude) mice with OBLV60 and assessing viral clearance with plaque assays and in situ hybridization (Fig. 3B and 5). These mice failed to clear the virus and were moribund between 11 and 16 days postinfection. Infected neurons could be demonstrated in these mice in many regions including the cerebellum, which was not infected in immune-competent mice (Fig. 6). Thus, T cells were important in clearing the virus from the CNS. To determine the relative contribution of T-cell subsets in this process we selectively depleted mice of CD4$^+$ cells, CD8$^+$ cells, or both and then infected these mice with OBLV60. In situ hybridization revealed that both T-cell subsets are necessary for optimal clearance, since viral RNA could be detected at 11 days postinfection in the brains of mice depleted of either CD4$^+$ or CD8$^+$ cells (Fig. 7). Infection with OBLV60 appeared to result in loss of mitral cells in immunocompetent mice as well as in mice depleted of CD4$^+$ or CD8$^+$ cells (Fig. 8). Simultaneous depletion of both CD4$^+$ and CD8$^+$ T-cell subsets resulted in dissemination of virus throughout numerous brain regions, including the cerebellum (Fig. 7). Virus could be detected by plaque assay from the brains of CD4$^+$ cell-depleted mice but not from the brains of CD8$^+$ cell-depleted mice at 16 days postinoculation (Table 1). Virus persisted in the brains, but not in the olfactory bulbs, of CD4$^+$ cell-depleted mice at 31 days postinfection, yet these mice appeared normal clinically.

To investigate the mechanism by which T cells mediated clearance, we performed immunohistochemical analyses for CD4$^+$ and CD8$^+$ cells on OBLV60-infected brain tissue at 6 days postinfection, when T-cell-mediated clearance was maximal (Fig. 9). In uninfected brain tissues (Fig. 9B and D), only one or two cells expressing either marker were observed in each sagittal section, usually in the choroid plexus or ependyma. In contrast, brain tissue from OBLV60-infected BALB/c mice consistently had numerous CD4$^+$ (Fig. 9A) and CD8$^+$ (Fig. 9C) cells in the olfactory bulb and the brain stem. The common appearance of these cells near vessels indicated they had probably infiltrated into the brain from the bloodstream. Whereas most CD4$^+$ and CD8$^+$ cells were predominantly found in regions which were infected, there was a general increase in these cells near vessels and in the choroid plexus, ependyma, and meninges. Occasionally, stained cells were found in regions not usually infected, such as the hippocampus. Cells expressing CD8 were more widespread than those expressing CD4. In the olfactory bulb, both CD4$^+$ and CD8$^+$ cells were observed in the internal granule layer (Fig. 9A and C), even though this layer has very few infected cells compared with the mitral or glomerular layers (Fig. 2). The role of these lymphocytes in the internal granule layer is undetermined; a mild necrosis in this region is observed even when mice are depleted of either CD4$^+$ or CD8$^+$ cells (Fig. 8).

Surprisingly, in nude mice CD4$^+$ cells were observed in the olfactory bulb and surrounding meninges (data not shown). CD4$^+$ cells were very rare outside the olfactory bulb or immediately adjacent areas in nude mice. Cells staining for the CD8 marker could also be found in the olfactory bulb region of nude mice, although they were rare in comparison to their frequency in the olfactory bulbs of infected immune-competent mice. Unlike infected immunocompetent mice, the brains of infected nude mice usually had no CD8$^+$ cells outside the olfactory bulb region.

Immunohistochemical analysis with MAb F4/80 (53) was used to determine if macrophages and activated microglia

FIG. 4. In situ hybridization showing the effect of immune suppression on clearance of OBLV60. Sagittal brain sections from: a normal mouse at 11 days after infection (A); a mouse treated with 5 mg of cyclophosphamide intraperitoneally on the day of inoculation and again at 5 days after inoculation and then sacrificed at 11 days (B); and a mouse treated with 5 mg of cyclophosphamide intraperitoneally at 24 days after inoculation and then sacrificed at 31 days postinoculation.

were present during clearance (Fig. 9E, F, and G). Macrophages were observed in infected regions, and there was an increased staining intensity even in regions where infected cells were uncommon (Table 2). Many stained cells were morphologically similar to ramified microglia. There was a fine reticular staining which manifested no overt regional localization in uninfected brain tissue but which was intensified and appeared as microglial profiles in the brain tissue of infected mice. This staining enhancement was particularly evident in infected regions. The pattern of staining in nude and BALB/c mice was similar at 6 days postinfection. Astrocytosis was limited to infected regions in BALB/c and nude mice (Table 2).

Although virus was cleared by 11 days after infection in normal mice, F4/80 staining remained elevated at 26 days (Table 2). Nude mice died prior to this time, but there was intense staining throughout their brain tissue at 11 days (Table 2).

It has been proposed that cytokines mediate clearance of viruses from the CNS (54). In the brain, cytokines may be produced by infiltrating immune cells, microglia, or astrocytes (5). The infiltration of macrophages and CD4$^+$- and CD8$^+$-positive cells, as well as the activation of microglia and astrocytes, all of which occurred during OBLV60 clearance, prompted us to investigate cytokine induction during viral clearance. For this purpose we used an RNase protection assay to measure cytokine transcripts for IL-1$\alpha$, IL-1$\beta$, IL-2, IL-3, IL-4, IL-5, IL-6, tumor necrosis factor alpha (TNF-$\alpha$), TNF-$\beta$, and IFN-$\gamma$. In the brains of BALB/c mice there was an abrupt increase in mRNA for TNF-$\alpha$, IL-1$\alpha$ and -$\beta$, IL-6, and INF-$\gamma$, which corresponded to the time of maximal clearance (Fig. 10). These cytokines returned to baseline as the virus was cleared. In the brains of nude mice 6 days after inoculation, these cytokines were similarly induced, with the exception of IFN-$\gamma$ which was barely detectable (Fig. 11). Nude mice did not clear



**3 Days Post Infection**

**5 Days Post Infection**

**7 Days Post Infection**
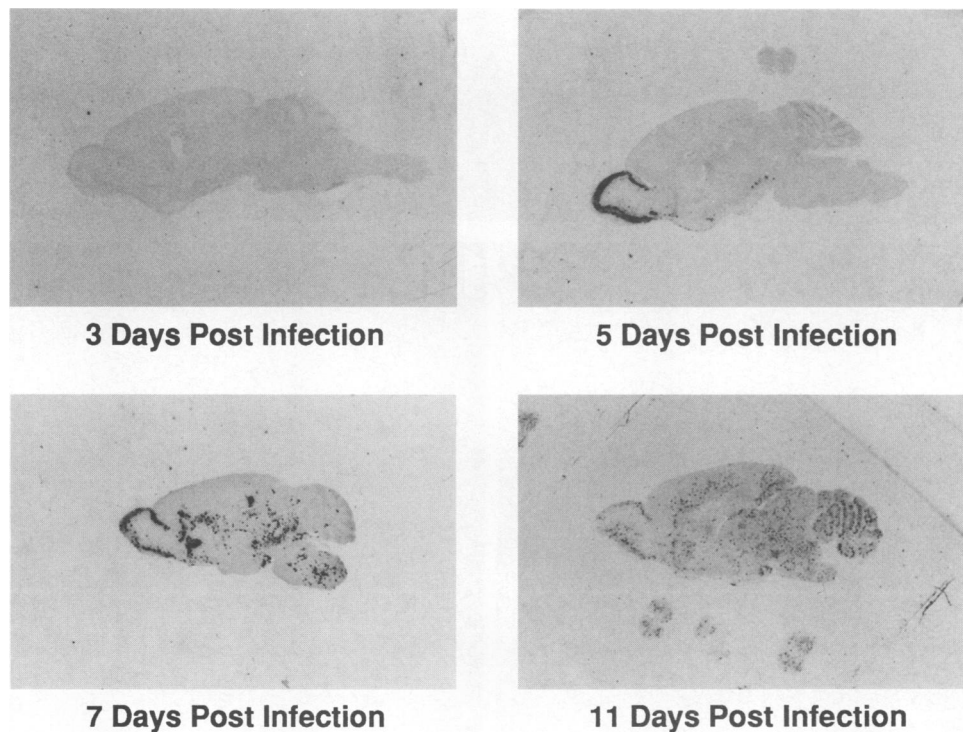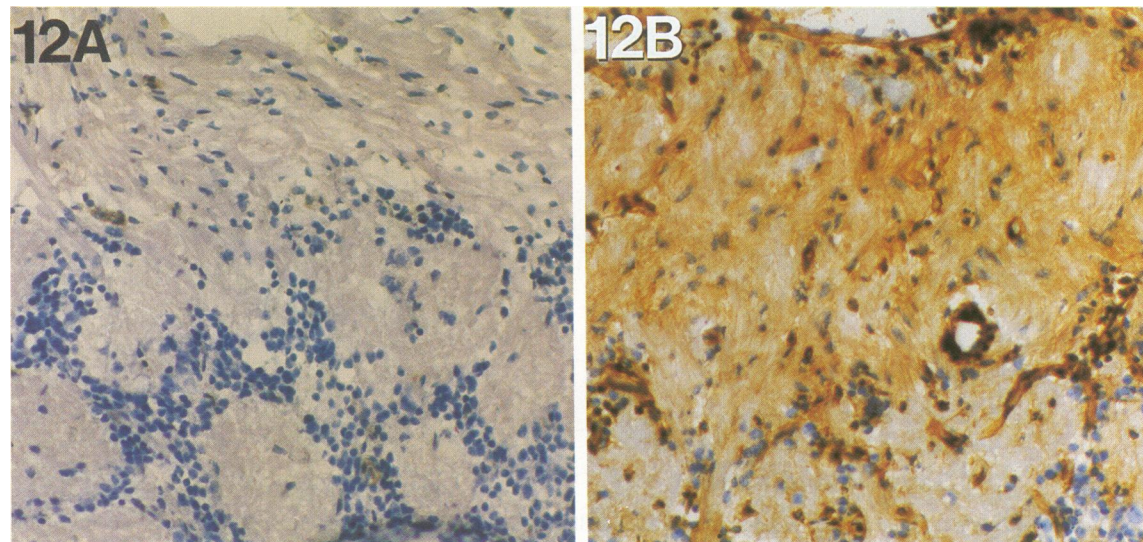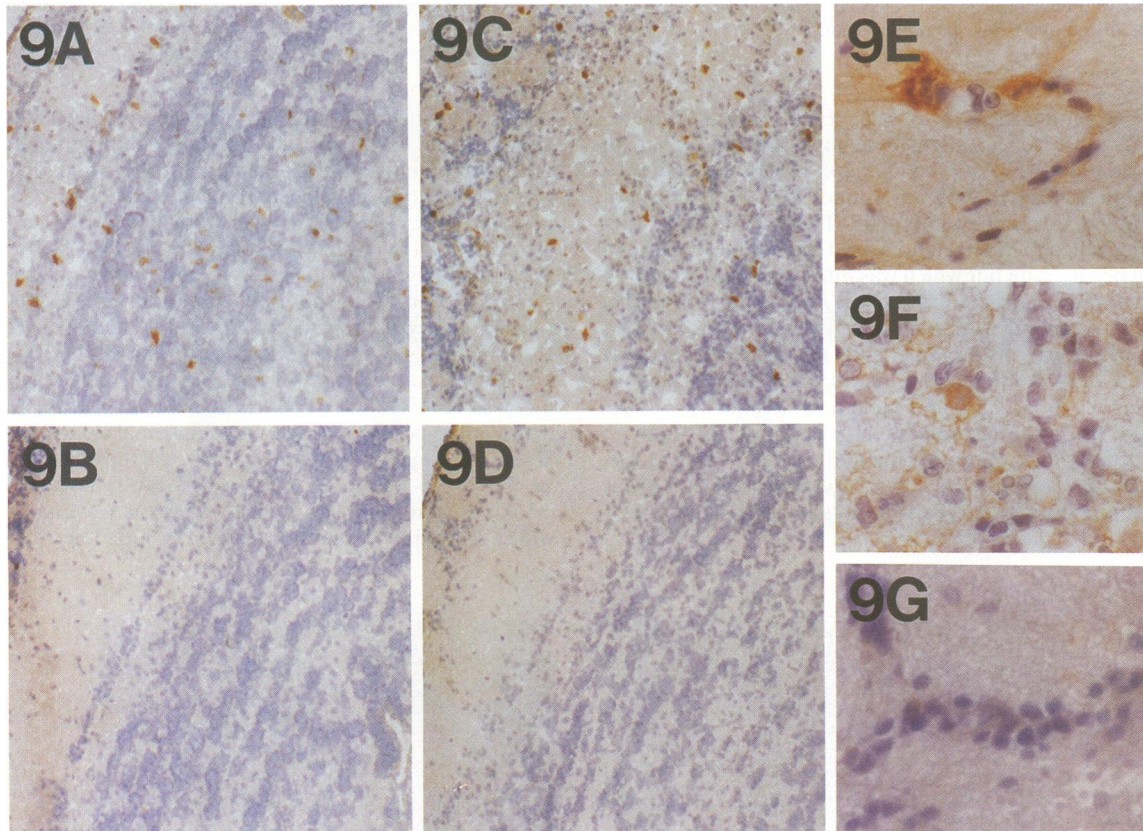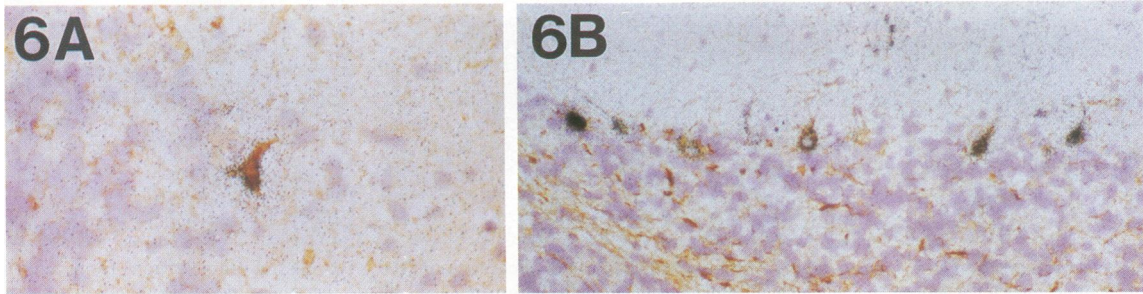
**11 Days Post Infection**

FIG. 5. In situ hybridization for viral RNA showing the spread of OBLV60 in the CNS of nude mice. Note disseminated infection in the brain and spinal cord at 11 days postinfection.

the virus (Fig. 3B and 5), and their cytokine transcripts remained elevated at 11 days (Fig. 11).

During clearance of viral infection, elements of the immune system work in concert. The presence of CD8$^+$ cell infiltrates in infected brains suggested that CTL-mediated events may be operating within the CNS during clearance of OBLV60 infection. An important component of CTL-mediated immunity is the expression of MHC-I molecules which is normally very low in the brain. Given the induction of IFN-$\gamma$ and TNF-$\alpha$ during clearance of OBLV60 and the known role of these cytokines in upregulating MHC-I expression on neural cells (5), we investigated whether MHC-I expression was induced concomitant with the clearance of OBLV60. Immunohistochemical analysis with an antibody against H-2 monotypic antigen of MHC-I demonstrated a large increase in MHC-I expression in the brains of mice 6 days after infection with OBLV60 (data not shown). There was a generalized increase in the staining of vessels throughout the brain, but this was particularly evident in infected regions like the olfactory bulb. Some of the intense staining in the olfactory bulb was not associated with vessels. Staining with an $H$-$2K^d$-specific antibody gave similar results, although staining extraneous to vessels was more evident, especially in the outer layers of the olfactory bulb, including the nerve fiber layer (Fig. 12). Staining remained increased in the olfactory bulb 26 days after infection (Table 2). There were similar increases in $H$-$2K^d$ in the brains of nude mice 6 days after infection. By 11 days postinfection, $H$-$2K^d$ staining was found throughout the brains of nude mice, including the hippocampus, although the most intense staining was in the olfactory bulb which had been infected the longest (Table 2). In situ hybridization revealed that many brain regions were infected at this time, although the hippocampus was usually uninfected or only sparsely infected (Fig. 5).

Immunohistochemical analyses for MHC-II ($IA^d$) of brain tissues from BALB/c mice at 6 days postinfection revealed a small number of positive cells which were clustered in the glomerular and external plexiform layers of the olfactory bulb (Table 2). The morphology of these cells was consistent with that of lymphocytes although they were slightly less common, and their infiltration apparently less extensive, than cells staining for either CD4 or CD8.

## DISCUSSION

We have developed an in vivo mouse model, utilizing infection with the OBLV60 variant of MHV, which has several features that make it advantageous for the study of clearance mechanisms. (i) The virus is neuroinvasive: we obtain consistent and reproducible CNS infection with OBLV60 by intra- nasal administration. This obviates the localized CNS trauma associated with intracranial inoculations. (ii) The virus is neuronotropic but is neuroattenuated: OBLV60 infects neurons and grows to high titers in the olfactory bulb, yet there is virtually no mortality in mice given 1,000 PFU intranasally. Thus, the clearance of OBLV60 from neurons can be investigated with little risk of mice dying of encephalitis. (iii) Clearance of virus occurs rapidly and is complete by 11 days after inoculation. Although many strains of MHV produce paralytic disease after recovery from the acute infection (12, 16, 38, 40), this is not observed with OBLV60.

Using this model we have determined that both CD4$^+$ and CD8$^+$ subsets play an important role in clearing OBLV60 from the brain. Normal BALB/c mice clear virus from the brain by 11 days, but nude mice are unable to do so and inevitably succumb to encephalitis. Our data are consistent with those of previous studies using other strains of MHV which have demonstrated the importance of T cells in mediating clearance or protecting mice from MHV-induced encephalitis (48, 63, 68, 71). Although the mechanism of clearance was not established by these prior studies, CTL-mediated lysis of infected cells has been suggested (71). Our data, as well as several prior studies (63, 67, 68, 71), could be interpreted to support this hypothesis. We found that clearance of OBLV60 is delayed in mice depleted of CD8$^+$ T cells, and mice infected with OBLV60 had CD8$^+$ cell infiltration and upregulation of MHC-I in infected regions of their brains at a time which coincided with maximal viral clearance. Nevertheless, if immunocompetent mice cleared the virus primarily through CTL-mediated lysis of infected cells then, given the large number of infected cells in the olfactory bulb, we would have expected to observe considerably more destruction in the olfactory bulbs of these mice during clearance than in the olfactory bulbs of mice depleted of CD8$^+$ cells. The degree of cell destruction did not appear to be reduced in olfactory bulbs taken from infected mice depleted of CD8$^+$ cells compared with those of infected controls. Therefore, CD8$^+$ cells may be operating to clear virus through nonlytic mechanisms. Ultimately, CD8$^+$ cells may not be strictly essential for clearance because all mice depleted of these cells cleared the virus by 16 days postinfection.

In contrast, mice depleted of CD4$^+$ cells were persistently infected and virus could be recovered from their brains at 31 days postinfection. Previous studies have demonstrated the importance of CD4$^+$ cells in clearance of MHV from the mouse CNS (48, 63, 68). One mechanism suggested is that CD4$^+$ cells may provide help to CD8$^+$ effectors, and it is presumably these CD8$^+$ effectors which clear the virus through lysis of infected cells. Alternatively, CD4$^+$ cells may release

FIG. 6. Infected neurons in brain sections from athymic nude mice at 11 days postinfection, as demonstrated by combined immunohistochemistry for neurofilament protein and in situ hybridization for viral RNA. (A) Infected neuron in mitral cell layer of olfactory bulb. (B) Infected Purkinje cells in the cerebellum. Neurons and their processes are stained brown and are identified as being infected by the overlying black grains from in situ hybridization. Original magnification, ×400 (panel A); ×200 (panel B).

FIG. 9. Immunostaining for CD4 (A and B) or CD8 (C and D) in the olfactory bulb of mice 6 days after intranasal infection with OBLV60 (A and C) or in sham-inoculated controls (B and D). Note infiltrates of CD4$^+$ and CD8$^+$ cells in tissue from infected mice only. Typical results of staining for macrophages and microglia, using the MAb F4/80, are shown in the olfactory bulbs of an infected immunocompetent mouse (E), infected nude mouse (F), and uninfected immunocompetent mouse (G). Each experiment included controls for specificity of staining, in which the primary antibody was omitted. Original magnification, ×100 (panels A through D); ×600 (panels E through G).

FIG. 12. Induction of $H$-$2K^d$ immunoreactivity in the olfactory bulb by intranasal infection with OBLV60 at 6 days postinfection. (A) Section from a sham-infected mouse showing minimal staining in the glomerular and nerve fiber layers. (B) Section from a comparable region of an OBLV60-infected mouse showing intense parenchymal and perivascular staining. Staining was specific since no staining was observed when the primary MAb ($H$-$2K^d$) was replaced with a MAb against a mismatched H-2 antigen ($H$-$2K^b$). Original magnification, ×200.
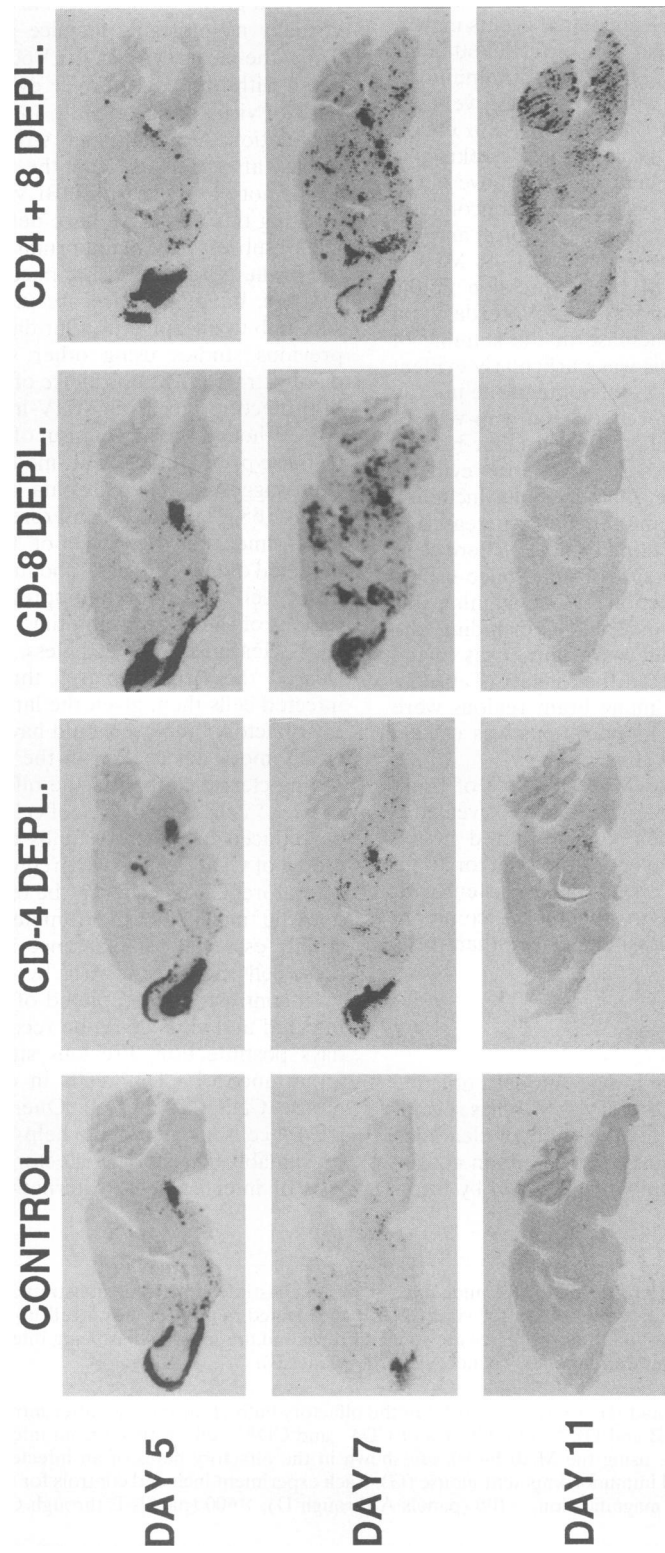
FIG. 7. In situ hybridization for viral RNA showing that depletion of $CD4^+$ cells, $CD8^+$ cells, or both T-cell subsets delays clearance of OBLV60. All inoculations were intranasal; the number of days postinoculation is on the left.
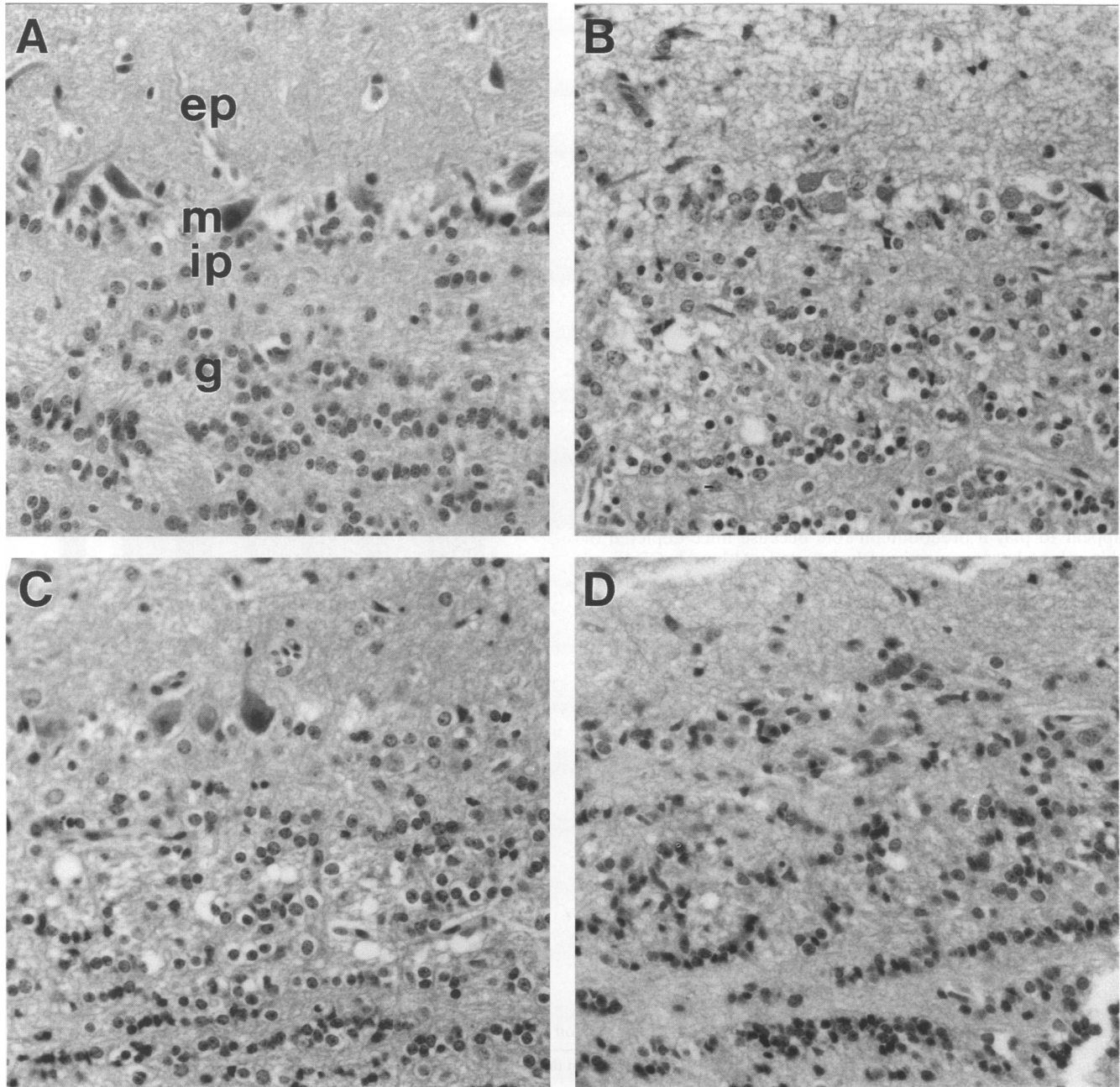
FIG. 8. Histopathologic changes in the olfactory bulb 11 days after infection with OBLV60. (A) Uninfected control. (B) Immunocompetent mouse intranasally infected with OBLV60. (C) CD4$^+$ cell-depleted mouse intranasally infected with OBLV60. (D) CD8$^+$ cell-depleted mouse intranasally infected with OBLV60. Note cell loss in the mitral cell layer in immunocompetent mice as well as in mice depleted of T-cell subsets. Mild necrosis and mononuclear cell infiltration are seen in the internal granule layer. ep, external plexiform; m, mitral; ip, internal plexiform; g, internal granule layer. Hematoxylin and eosin stain. Original magnification, ×200.

cytokines which act on infected cells to mediate clearance (48, 66).

Whereas numerous cytokines have been reported to be induced by MHV (20, 29, 31, 37, 43, 44, 48, 58, 61, 65, 66), a clear picture of which cytokines are essential for mediating viral clearance in vivo has not emerged. Therefore, to identify which cytokines may play an essential role in virus clearance, we compared the mRNA induction patterns for 10 cytokines in the brains of immunocompetent BALB/c mice infected with

OBLV60. We found induction of IL-1α, IL-1β, IL-6, TNF-α and IFN-γ in immune-competent mice at 6 days postinfection during the period of maximal clearance. In nude mice a similar pattern of induction was found at this time, with the exception of mRNA for IFN-γ which was barely detected. In view of the well-documented antiviral properties of IFN-γ, the data suggest a possible role of this cytokine in mediating virus clearance from the CNS. Nevertheless, other cytokines implicated in antiviral immune responses may also be important. For future

TABLE 1. Percentage of mice from which virus could be recovered after depletion of T-cell subsets

| | % of mice from which virus was recovered | | | |
| | 16 days postinfection | | 31 days postinfection | |
| | CD4 depleted | CD8 depleted | CD4 depleted | CD8 depleted |
| --- | --- | --- | --- | --- |
| Olfactory bulb | 17[a] | 0 | 0 | ND[b] |
| Remainder of brain | 100[c] | 0 | 100[d] | ND |

[a] Average titer (PFU per g of tissue) was $2.3 \times 10^2$.
[b] ND, not done.
[c] Average titer (PFU per g of tissue) was $3.7 \times 10^2$.
[d] Average titer (PFU per g of tissue) was $1.7 \times 10^4$.

studies, it will be useful to design an RNase protection assay to detect additional transcripts for antiviral cytokines, such as IL-12, IFN-β, and granulocyte-macrophage colony-stimulating factor, and to correlate the observed message levels with cytokine concentrations in tissues.

Both CD4$^+$ and CD8$^+$ cells can produce IFN-γ in response to MHV (48, 71). Whereas IFN-γ production by either subset would be consistent with our findings in nude mice, CD4$^+$ cells appear to play a predominant role because mice depleted of this subset become persistently infected. Although CD4 and CD8 immunoreactive cells were found in the olfactory bulbs of nude mice infected with OBLV60, these cells were ineffective in mediating clearance, perhaps because these T cells were too scarce, immature, or had not undergone clonal expansion in response to the virus (32, 35).

The induction of mRNA for IL-1, IL-6, and TNF-α at 6 days was comparable in nude mice and immunocompetent BALB/c mice. In the CNS, these and other cytokines mediate communication between resident and infiltrating cells through a complex network in which immune accessory molecules such as MHC and cytokine expression are interregulated in response to infection. As an element in this network, TNF-α may be acting synergistically with IFN-γ to mediate clearance (14, 57, 70). IFN-γ can also act synergistically with IL-1 or TNF to induce nonimmune cells to produce manganese superoxide dismutase which protects against oxygen-free radicals (23, 69). Considering that IL-1, TNF-α, and IL-6 are known mediators of CNS damage (5), the coinduction of IFN-γ with these
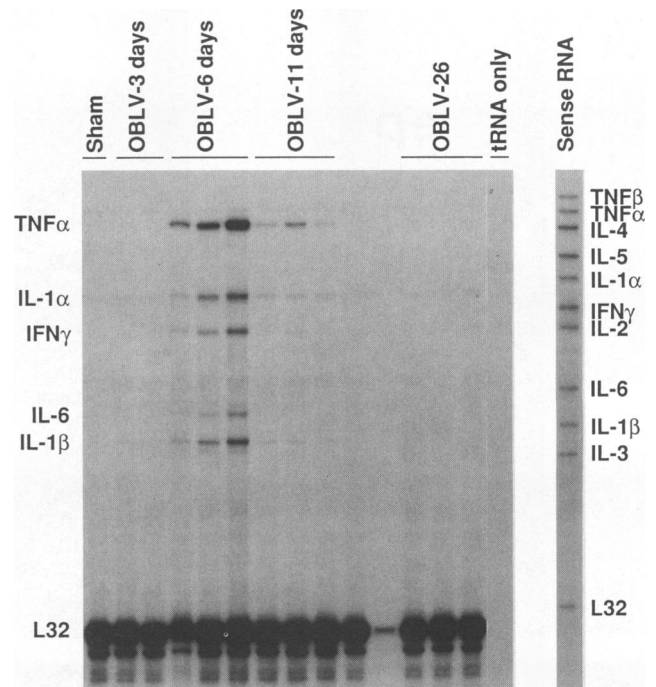


FIG. 10. RNase protection assay measuring induction of cytokine mRNA after intranasal inoculation with OBLV60. RNA was extracted from the brain tissues of BALB/c mice at various times after infection and then hybridized with a $^{32}$P-labeled antisense probe-set designed to detect 10 different cytokine transcripts. A probe for L32 was included in the probe set to verify consistency in loading and assay performance. After separation by polyacrylamide gel electrophoresis, protected probe fragments were visualized by autoradiography. All assays included a sample consisting of a set of sense RNAs complementary to the probe set for use in standardization of fragment size and assay integrity. These sense RNAs contain cloning sequences and consequently run slightly higher than protected fragments from brain RNA. Controls included tRNA only and RNA from the brain of a sham-infected mouse.

TABLE 2. Results of immunohistochemical analyses on brain sections after intranasal infection with OBLV60

| Mouse | Day postinfection | Cell type (identifying antigen) and location during viral clearance[a] | | | | | | MHC expression (identifying antigen) and location during viral clearance | | | | | |
| | | Microglia/macrophage (F4/80)[b] | | | Astrocyte (GFAP) | | | MHC-I (H-2K$^d$) | | | MHC-II (IA$^d$) | | |
| | | Olf.B | Hipp | Cerebell | Olf.B | Hipp | Cerebell | Olf.B | Hipp | Cerebell | Olf.B | Hipp | Cerebell |
| --- | --- | --- | --- | --- | --- | --- | --- | --- | --- | --- | --- | --- | --- |
| BALB/c | | | | | | | | | | | | | |
| | 3 | − | − | − | ND | ND | ND | − | − | − | ND | ND | ND |
| | 6 | ++++ | −/+ | − | ++ | − | − | ++++ | − | − | + | − | − |
| | 11 | ++++ | ++ | −/+ | ND | ND | ND | +++ | −/+ | −/+ | ND | ND | ND |
| | 26 | +++ | + | − | ND | ND | ND | ++ | − | − | ND | ND | ND |
| Nude | | | | | | | | | | | | | |
| | 3 | ND | ND | ND | ND | ND | ND | −/+ | − | − | ND | ND | ND |
| | 6 | ++++ | + | − | ++ | − | − | ++++ | − | − | ND | ND | ND |
| | 11 | ++++ | +++ | +++ | ND | ND | ND | ++++ | ++ | + | ND | ND | ND |

[a] Olf.B, olfactory bulb; Hipp, hippocampus; Cerebell, cerebellum.
[b] Degree of increased staining intensity relative to uninfected controls: −, none; −/+, slight increase observed in most sections; +, mild increase seen consistently, ++, moderately increased staining, easily recognizable positive reaction, +++, large increase in intensity of staining; ++++, equivalent to highest intensity of staining observed. ND, not done.
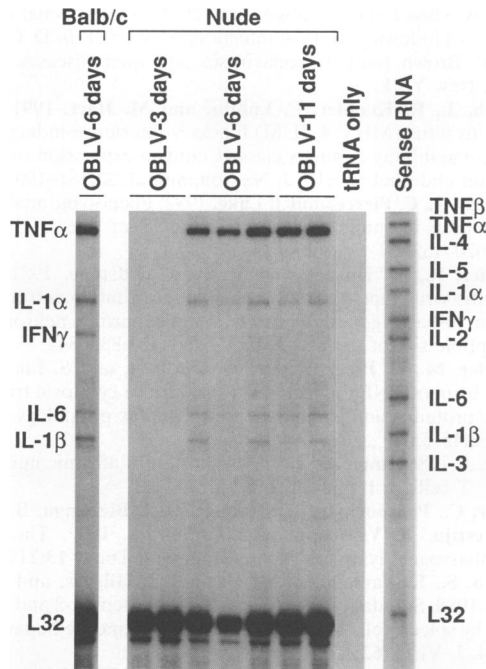
FIG. 11. RNase protection assay comparing the effects of intranasal infection with OBLV60 in immunocompetent (BALB/c) and athymic nude mice on the induction of cytokine mRNA. Methods were as described in the legend to Fig. 10.

monokines may attenuate their deleterious effects on neural cells. Both IL-1 and TNF-α are known to be produced as precursor proteins (21, 24, 34), and IL-6 production is not exclusively under transcriptional control (29). Therefore, whereas our RNase protection assay gave an indication of which cytokines were induced during infection, the activity of these proteins may also be modulated by posttranscriptional events.

In vitro, MHC-I expression in cells derived from the brain can be increased, decreased, or unchanged by infection with MHV, depending on cell type, MHC haplotype, and host species (30, 46, 64). Induction of MHC-I mRNA has been reported in mouse brain tissue after infection with MHV-A59 (22). Consistent with these RNA data, we found by immunostaining that MHC-I was induced in the brain by infection with OBLV60. Considered in the context of cytokine induction in our mice, several conclusions can be put forth from these data. (i) Although the greatest increase in MHC-I was in infected regions, the increased immunostaining in adjacent uninfected regions suggests that a soluble factor(s) mediates induction. (ii) Although IFN-γ has been proposed as a mediator of MHC-I upregulation in response to MHV infection (59, 66, 71), we found that MHC-I induction by OBLV60 was similar in normal and nude mice and hence was not quantitatively dependent on IFN-γ induction. The suggestion that a soluble factor like TNF may mediate MHC-I induction on glia (64) is consistent with our finding that mRNA for TNF-α was comparably induced in normal and nude mice. IFN-α/β can also induce MHC-I expression in the periphery (42), and circulating levels of IFN-α/β are increased after infection with MHV (20). (iii) Immunostaining for MHC-I remained elevated at least 15 days after the virus was cleared, perhaps because mRNA levels for MHC remained elevated as indicated by studies with MHV-A59 (22). (iv) Upregulation of MHC-I in

the nerve fiber layer of the olfactory bulb suggests that some neurons may be capable of MHC-I antigen presentation, as suggested by recent in vitro and in vivo studies (11, 28, 45).

Whereas an understanding of the exact mechanism by which OBLV60 is cleared will require further study, on the basis of our data and hypotheses derived from studies with other viruses, the following scheme is proposed. OBLV60 initially infects the nasal mucosa and enters the olfactory bulb by axonal transport along the olfactory nerve (1, 2, 39). Primary immune activation likely occurs in cervical lymph nodes (4, 10) or nasal-associated lymphatic tissue (36), and between 3 and 6 days after infection monokines are produced by invading macrophages, endothelial cells, and glia (5, 6, 8, 18, 29). T cells infiltrate the brain by 6 days, perhaps because of the expression of adhesion molecules on endothelial surfaces induced by TNF-α and IL-1 (60). Expression of MHC-I on the endothelium may also be important for extravasation of CD8 T cells (30, 59), and parenchymal MHC-I expression could activate T cells and focus antiviral cytokine production at sites of infection (54). While some neurons might be cleared of virus, others could be killed either by the immune response or by the cytopathic effects of the virus itself. Additional studies are needed to determine which of these mechanisms predominates.

## REFERENCES

1. **Barnett, E., and S. Perlman.** 1993. The olfactory nerve and not the trigeminal nerve is the major site of CNS entry for mouse hepatitis virus, strain JHM. Virology **194:**185–191.
2. **Barthold, S.** 1988. Olfactory neural pathway in mouse hepatitis virus nasoencephalitis. Acta Neuropathol. **76:**502–506.
3. **Barthold, S., and A. Smith.** 1990. Duration of mouse hepatitis virus infection: studies in immunocompetent and chemically immunosuppressed mice. Lab. Anim. Sci. **40:**133–137.
4. **Barthold, S., and A. Smith.** 1992. Viremic dissemination of mouse hepatitis virus-JHM following intranasal inoculation of mice. Arch. Virol. **122:**35–44.
5. **Benveniste, E.** 1992. Inflammatory cytokines within the central nervous system: sources, function, and mechanism of action. Am. J. Physiol. **263:**1–16.
6. **Benveniste, E., S. Sparacio, J. Norris, H. Grenett, and G. Fuller.** 1990. Induction and regulation of interleukin-6 gene expression in rat astrocytes. J. Neuroimmunol. **30:**201–212.
7. **Buchmeier, M., R. Dalziel, and M. Koolen.** 1988. Coronavirus-induced CNS disease: a model for virus-induced demyelination. J. Neuroimmunol. **20:**111–116.
8. **Chung, I., and E. Benveniste.** 1990. Tumor necrosis factor-α production by astrocytes: induction by lipopolysaccharide, IFN-γ, and IL-1β. J. Immunol. **144:**2999–3007.
9. **Compton, S., S. Barthold, and A. Smith.** 1993. The cellular and molecular pathogenesis of coronaviruses. Lab. Anim. Sci. **43:**15–28.
10. **Cserr, H., and P. Knopf.** 1992. Cervical lymphatics, the blood-brain barrier and the immunoreactivity of the brain: a new view. Immunol. Today **13:**507–512.
10a.**de Souza, M., A. Smith, and K. Bottomly.** 1991. Infection of Balb/cByJ mice with the JHM strain of mouse hepatitis virus alters in vitro splenic T cell proliferation and cytokine production. Lab. Anim. Sci. **41:**99–105.

11. **Duguid, J., and C. Trzepacz.** 1993. Major histocompatibility complex genes have an increased brain expression after scrapie infection. Proc. Natl. Acad. Sci. USA **90:**114–117.

12. **Dupuy, J., C. I. Prevost, E. Levy-Leblond, and J. Virelizier.** 1973. Persistent virus infection with neurological involvement in mice infected with MHV3. Fed. Proc. **32:**963.

12a.**Fazakerley, J., and M. Buchmeier.** Unpublished observations.

13. **Fazakerley, J., S. Parker, F. Bloom, and M. Buchmeier.** 1992. The V5A13.1 envelope glycoprotein deletion mutant of mouse hepatitis virus type-4 is neuroattenuated by its reduced rate of spread in the central nervous system. Virology **187:**178–188.

14. **Feduchi, E., M. A. Alonso, and L. Carrasco.** 1989. Human gamma interferon and tumor necrosis factor exert a synergistic blockade on the replication of herpes simplex virus. J. Virol. **63:**1354–1359.

15. **Fleming, J., M. Trousdale, J. Bradbury, S. Stohlman, and L. Weiner.** 1987. Experimental demyelination induced by coronavirus JHM (MHV-4): molecular identification of a viral determinant of paralytic disease. Microb. Pathol. **3:**9–20.

16. **Fleming, J., F. Wang, M. Trousdale, D. Hinton, and S. Stohlman.** 1990. Immunopathogenesis of demyelination induced by MHV-4, p. 565–572. In D. Cavanagh and T. Brown (ed.) Coronaviruses and their diseases. Plenum Press, New York.

17. **Fleming, J. O., M. D. Trousdale, F. A. K. El-Zaatari, S. A. Stohlman, and L. P. Weiner.** 1986. Pathogenicity of antigenic variants of murine coronavirus JHM selected with monoclonal antibodies. J. Virol. **58:**869–875.

18. **Frei, K., U. Malipiero, T. Leist, R. Zinkernagel, M. Schwab, and A. Fontana.** 1989. On the cellular source and function of interleukin 6 produced in the central nervous system in viral diseases. Eur. J. Immunol. **19:**689–694.

19. **Gallagher, T. M., C. Escarmis, and M. J. Buchmeier.** 1991. Alteration of the pH dependence of coronavirus-induced cell fusion: effect of mutations in the spike glycoprotein. J. Virol. **65:**1916–1928.

20. **Garlinghouse, L., and A. Smith.** 1985. Responses of mice susceptible or resistant to lethal infection with mouse hepatitis virus, strain JHM, after exposure by a natural route. Lab. Anim. Sci. **35:**469–472.

21. **Giri, J., P. Lomedico, and S. Mizel.** 1985. Studies on the synthesis and secretion of interleukin 1: a 33,000 molecular weight precursor for interleukin 1. J. Immunol. **134:**343–349.

22. **Gombold, J., and S. Weiss.** 1992. Mouse hepatitis virus A59 increases steady-state levels of MHC mRNAs in primary glial cell cultures and in the murine central nervous system. Microb. Pathog. **13:**493–505.

23. **Harris, C., K. Derbin, B. Hunte-McDonough, M. Krauss, K. Chen, D. Smith, and L. Epstein.** 1991. Manganese superoxide dismutase is induced by IFN-γ in multiple cell types. J. Immunol. **147:**149–154.

24. **Hazdua, D., J. Strickler, F. Kueppers, P. Simon, and P. Young.** 1990. Processing of precursor interleukin 1β and inflammatory disease. J. Biol. Chem. **265:**6318–6322.

25. **Hobbs, M., W. Weigle, D. Noonan, B. Torbett, R. McEvilly, R. Koch, G. Cardenas, and D. Ernst.** 1993. Patterns of cytokine gene expression by CD4+ T cells from young and old mice. J. Immunol. **150:**3602–3614.

26. **Hofler, H., B. Putz, C. Ruhri, G. Wirnsberger, M. Klimpfinger, and J. Smolle.** 1987. Simultaneous localization of calcitonin mRNA and peptide in a medullary thyroid carcinoma. Virchows Arch. B Cell Pathol. **54:**144–151.

27. **Iwasaki, Y., N. Hirano, T. Tsukamoto, and S. Haga.** 1990. Vacuolar degeneration induced by JHM-CC virus in the CNS of cyclophosphamide-treated mice, p. 601–607. In D. Cavanagh and T. Brown (ed.), Coronaviruses and their diseases. Plenum Press, New York.

28. **Joly, E., L. Mucke, and M. B. A. Oldstone.** 1991. Viral persistence in neurons explained by lack of major histocompatibility class I expression. Science **253:**1283–1285.

29. **Joseph, J., J. Grun, F. Lublin, and R. Knobler.** 1993. Interleukin-6 induction in vitro in mouse brain endothelial cells and astrocytes by exposure to mouse hepatitis virus (MHV-4, JHM). J. Neuroimmunol. **42:**47–52.

30. **Joseph, J., R. Knobler, F. Lublin, and M. Hart.** 1990. Regulation of MHC class I and II antigens on cerebral endothelial cells and astrocytes following MHV-4 infection, p. 579–591. In D. Cavanagh and T. Brown (ed.), Coronaviruses and their diseases. Plenum Press, New York.

31. **Joseph, J., R. Knobler, F. Lublin, and M. Hart.** 1991. Mouse hepatitis virus (MHV-4, JHM) blocks γ-interferon-induced major histocompatibility complex class II antigen expression on murine cerebral endothelial cells. J. Neuroimmunol. **33:**181–190.

32. **Kennedy, J., C. Pierce, and J. Lake.** 1992. Phenotypic analysis of T cell subsets in nude mice as a function of age. J. Immunol. **148:**1620–1629.

33. **Knobler, R., M. Haspel, and M. B. A. Oldstone.** 1981. Mouse hepatitis virus type 4 (JHM strain)-induced fatal central nervous system disease: genetic control and the murine neuron as the susceptible site of disease. J. Exp. Med. **153:**832–843.

34. **Kriegler, M., C. Perez, K. DeFay, I. Albert, and S. Lu.** 1988. A novel form of TNF/cachectin is a cell surface cytotoxic transmembrane protein: ramifications for the complex physiology of TNF. Cell **53:**45–53.

35. **Kung, J.** 1988. Impaired clonal expansion in athymic nude CD8+ CD4− T cells. J. Immunol. **140:**3727–3735.

36. **Kuper, C., P. Koornstra, D. Hameleers, J. Biewenga, B. Spit, A. Duijvestijn, P. Vriesman, and T. Sminia.** 1992. The role of nasopharyngeal lymphoid tissue. Immunol. Today **13:**219–224.

37. **Kyuwa, S., K. Yamaguchi, M. Hayami, J. Hilgers, and K. Fujiwara.** 1988. Spontaneous production of interleukin-2 and interleukin-3 by spleen cells from mice infected with mouse hepatitis virus type 4. J. Virol. **62:**3506–3508.

38. **Lampert, P., J. Sims, and A. Kniazeff.** 1973. Mechanism of demyelination in JHM virus encephalomyelitis. Acta Neuropathol. **24:**76–85.

39. **Lavi, E., P. Fishman, M. Highkin, and S. Weiss.** 1988. Limbic encephalitis after inhalation of a murine coronavirus. Lab. Invest. **58:**31–36.

40. **Lavi, E., D. Gilden, Z. Wroblewska, L. Rorke, and S. Weiss.** 1984. Experimental demyelination produced by the A59 strain of mouse hepatitis virus. Neurology **34:**597–603.

41. **Levine, B., J. Hardwick, B. Trapp, T. Crawford, R. Bollinger, and D. Griffin.** 1991. Antibody-mediated clearance of alphavirus infection from neurons. Science **254:**856–860.

42. **Lindahl, P., P. Leary, and I. Gresser.** 1973. Enhancement by interferon of the expression of surface antigens on murine leukemia L 1210 cells. Proc. Natl. Acad. Sci. USA **70:**2785–2788.

43. **Lucchiari, M., J. Martin, M. Modolell, and C. Pereira.** 1991. Acquired immunity of A/J mice to mouse hepatitis virus 3 infection: dependence on interferon-γ synthesis and macrophage sensitivity to interferon-γ. J. Gen. Virol. **72:**1317–1322.

44. **Lucchiari, M., M. Modolell, K. Eichmann, and C. Pereira.** 1992. In vivo depletion of interferon-γ leads to susceptibility of A/J mice to mouse hepatitis virus 3 infection. Immunobiology **185:**475–482.

45. **Maehlen, J., I. Nennesmo, A.-B. Olsson, T. Olsson, H. D. Schroder, and K. Kristensson.** 1989. Peripheral nerve injury causes transient expression of MHC class I antigens in rat motor neurons and skeletal muscles. Brain Res. **481:**368–372.

46. **Massa, P., R. Brinkmann, and V. ter Meulen.** 1987. Inducibility of Ia antigen on astrocytes by murine coronavirus JHM is rat strain dependent. J. Exp. Med. **166:**259–264.

47. **Mellon, P., J. Windle, P. Goldsmith, C. Padula, J. Roberts, and R. Weiner.** 1990. Immortalization of hypothalamic GnRH neurons by genetically targeted tumorigenesis. Neuron **5:**1–10.

48. **Mobley, J., G. Evans, M. Dailey, and S. Perlman.** 1992. Immune response to a murine coronavirus: identification of a homing receptor-negative CD4+ T cell subset that responds to viral glycoproteins. Virology **187:**443–452.

49. **Oldstone, M. B. A.** 1993. Viruses and diseases of the twenty-first century. Am. J. Pathol. **143:**1241–1249.

50. **Oldstone, M. B. A., P. Blount, P. Southern, and P. Lampert.** 1986. Cytoimmunotherapy for persistent virus infection reveals a unique clearance pattern from the central nervous system. Nature (London) **321:**239–243.

51. **Pasick, J., G. Wilson, V. Morris, and S. Dales.** 1992. SJL/J resistance to mouse hepatitis virus-JHM-induced neurologic disease can be partially overcome by viral variants of S and host

immunosuppression. Microb. Pathog. **13:**1–15.

52. **Patick, A., M. Lindsley, and M. Rodriguez.** 1990. Differential pathogenesis between mouse strains resistant and susceptible to Theiler's virus-induced demyelination. Semin. Virol. **1:**281–288.

53. **Perry, V., D. Hume, and S. Gordon.** 1985. Immunohistochemical localization of macrophages and microglia in the adult and developing mouse brain. Neuroscience **15:**313–326.

54. **Ramsay, A., J. Ruby, and I. Ramshaw.** 1993. A case for cytokines as effector molecules in the resolution of virus infection. Immunol. Today **14:**155–157.

55. **Ryder, E., E. Snyder, and C. Cepko.** 1990. Establishment and characterization of multipotent neural cell lines using retrovirus vector-mediated oncogene transfer. J. Neurobiol. **21:**356–375.

56. **Sambrook, J., E. Fritsch, and T. Maniatis.** 1989. Molecular cloning: a laboratory manual, 2nd ed. Cold Spring Harbor Laboratory Press, Cold Spring Harbor, N.Y.

57. **Schijns, V., R. van der Neut, B. Haagmans, D. Bar, H. Schellekens, and M. Horzinek.** 1989. Tumour necrosis factor-α, interferon-γ and interferon-β exert antiviral activity in nervous tissue cells. J. Gen. Virol. **72:**809–814.

58. **Schindler, L., H. Engler, and H. Kirchner.** 1982. Activation of natural killer cells and induction of interferon after injection of mouse hepatitis virus type 3 in mice. Infect. Immun. **35:**869–873.

59. **Sedgwick, J., and R. Dorries.** 1991. The immune system response to viral infection of the CNS. Semin. Neurosci. **3:**93–100.

60. **Sloan, D., M. Wood, and H. Charlton.** 1992. Leucocyte recruitment and inflammation in the CNS. Trends Neurosci. **15:**276–278.

61. **Smith, A., S. Barthold, M. de Souza, and K. Bottomly.** 1991. The role of gamma interferon in infection of susceptible mice with murine coronavirus, MHV-JHM. Arch. Virol. **121:**89–100.

62. **Stohlman, S., G. Matsushima, N. Casteel, and L. Weiner.** 1986. In vivo effects of coronavirus-specific T cell clones: DTH inducer cells prevent a lethal infection but do not inhibit virus replication. J. Immunol. **136:**3052–3056.

63. **Sussman, M. A., R. A. Shubin, S. Kyuwa, and S. A. Stohlman.** 1989. T-cell-mediated clearance of mouse hepatitis virus strain JHM from the central nervous system. J. Virol. **63:**3051–3056.

64. **Suzumura, A., E. Lavi, S. Bhat, D. Murasko, S. Weiss, and D. Silberberg.** 1988. Induction of glial cell MHC antigen expression in neurotropic coronavirus infection: characterization of the H-2-inducing soluble factor elaborated by infected brain cells. J. Immunol. **140:**2068–2072.

65. **Virelizier, J.-L., A.-M. Virelizier, and A. Allison.** 1976. The role of circulating interferon in the modifications of immune responsiveness by mouse hepatitis virus (MHV-3). J. Immunol. **117:**748–753.

66. **Williamson, J.** 1992. Virus-specific T cells in the central nervous system following infection with an avirulent neurotropic mouse hepatitis virus. Reg. Immunol. **4:**145–152.

67. **Williamson, J., K. Sykes, and S. Stohlman.** 1991. Characterization of brain-infiltrating mononuclear cells during infection with mouse hepatitis virus strain JHM. J. Neuroimmunol. **32:**199–207.

68. **Williamson, J. S. P., and S. A. Stohlman.** 1990. Effective clearance of mouse hepatitis virus from the central nervous system requires both CD4+ and CD8+ T cells. J. Virol. **64:**4589–4592.

69. **Wong, G., J. Elwell, L. Oberley, and D. Goeddel.** 1989. Manganous superoxide dismutase is essential for cellular resistance to cytotoxicity of tumor necrosis factor. Cell **58:**923–931.

70. **Wong, G., J. Krowka, D. Stites, and D. Goeddel.** 1988. In vitro anti-human immunodeficiency virus activities of tumor necrosis factor-α and interferon-γ. J. Immunol. **140:**120–124.

71. **Yamaguchi, K., N. Goto, S. Kyuwa, M. Hayami, and Y. Toyoda.** 1991. Protection of mice from a lethal coronavirus infection in the central nervous system by adoptive transfer of virus-specific T cell clones. J. Neuroimmunol. **32:**1–9.